Anuário do Instituto de Geociências
Universidade Federal do Rio de Janeiro
https://revistas.ufrj.br/index.php/aigeo/

ISSN 0101-9759
e-ISSN 1982-3908

Multipath Impact on Multi-Frequency and Multi-Constellation Code Measurements from Brazilian GNSS Stations

Impacto do Multicaminho em Observações Multifrequência e Multi-Constelações de Pseudodistância em Estações GNSS Brasileiras

Paulo T. Setti Jr.[1], Crislaine Menezes da Silva[2], Daniele Barroca Marra Alves[2], João Vitor Espinhosa Vieira[2] & João Pedro Voltare Zaupa[2]

[1]University of Luxembourg, Faculty of Science, Technology and Medicine, Esch-sur-Alzette, Luxembourg
[2]Universidade Estadual Paulista, Faculdade de Ciências e Tecnologia, Presidente Prudente, SP, Brasil

E-mail: paulo.setti@uni.lu; crislaine.menezes@unesp.br; daniele.barroca@unesp.br; joao.v.vieira@unesp.br; jp.zaupa@unesp.br
Corresponding author: Paulo T. Setti Jr.; paulo.setti@uni.lu

Abstract

Although Global Navigation Satellite Systems (GNSS) positioning can achieve high accuracy in line-of-sight conditions, multipath remains a dominant source of error. Multipath occurs when the reflected signals reach the receiver in addition to the direct ones. Different systems design can impact the multipath effect, such as the signal modulation and chipping rate. In the context of multi-frequency and multi-constellation scenario that we are achieving with four operational global constellations, this paper compares the multipath impact in different signals of GPS, GLONASS, Galileo and BeiDou. For the experiment, one week of data from 35 Brazilian Network for Continuous Monitoring of the GNSS Systems (RBMC) stations in June 2021 was processed. The multipath index was estimated based on the code-minus-carrier combination. For the first frequency of each system, similar results were obtained for GPS, GLONASS and BeiDou (approximately 56 cm). The Galileo BOC/AltBOC modulation offers better resistance to multipath, with a multipath index of 37 cm for E1 and of 12 cm for E5. Considering all selected stations, the multipath index of GPS L1 varied from 38 cm to 61 cm.

Keywords: RBMC; GLONASS; Galileo

Resumo

Embora o posicionamento pelos Sistemas Globais de Navegação por Satélite (GNSS) possa atingir alta acurácia em condições de visibilidade dos satélites, o multicaminho ainda é uma das principais fontes de erro. O multicaminho ocorre quando sinais refletidos chegam ao receptor em adição aos sinais diretos. Diferentes concepções dos sistemas podem impactar o efeito do multicaminho, como a modulação dos sinais e a taxa de chip. No contexto do cenário multi-frequência e multi-constelação que estamos atingindo com quatro constelações globais operacionais, esse trabalho compara o impacto do multicaminho nos diferentes sinais do GPS, GLONASS, Galileo e BeiDou. Para o experimento, uma semana de dados de 35 estações da Rede Brasileira de Monitoramento Contínuo dos Sistemas GNSS (RMBC) de junho de 2021 foi processada. O índice de multicaminho foi estimado com base na combinação código-menos-fase (CMC). Considerando a primeira frequência de cada sistema, resultados similares foram obtidos para os sistemas GPS, GLONASS e BeiDou (aproximadamente 56 cm). A modulação BOC/AltBOC do Galileo oferece maior resistência ao multicaminho, obtendo um índice de 37 cm para E1 e de 12 cm para E5. Considerando todas as estações selecionadas, o índice de multicaminho variou entre 38 cm e 61 cm para a frequência L1 GPS.

Palavras-chave: RBMC; GLONASS; Galileo

Received: 28 June 2022; Accepted: 11 February 2023

1 Introduction

Multipath is one of many error sources in Global Navigation Satellite Systems (GNSS) positioning. This effect occurs when one or more signals reflected from the ground or from the surrounding environment reach the receiver antenna, in addition to the direct line-of-sight signal (Seeber 2003). The properties of these signals are significantly different to the direct ones, covering a longer distance, reaching the receiver with a certain delay, and being in a different phase. These differences cause the amplitude of the wave to change and, as the receiver cannot always distinguish between the two of them, they interfere with each other and distort the direct signal. As a result, an error is added to the code and carrier-phase measurements, and the signal-to-noise ratio (SNR) parameter is affected (Braasch 2017).

Both carrier-phase and code measurements are affected by multipath propagation. While carrier-phase multipath errors range from millimeters to centimeters, the effect on pseudorange can go as high as 100 m in the most severe conditions (Seeber 2003). As it is a very localized effect, depending only on the local environment surrounding the antenna (Xu 2007), its impact cannot be eliminated by differential combinations or by universal models. Differential combinations increase the total impact of multipath error since the multipath from the reference station (and noises) are added to those of the user (Blunt 2009).

There are four main methods to avoid and/or mitigate the multipath error. The most obvious one is related to the antenna placement. The location for a permanent reference station, for example, should be chosen only after careful consideration of its surrounding, selecting a low or ideally multipath-free environment (Braasch 2017). The second one is related to the antenna type. The choke ring antenna, for example, consists of an antenna mounted inside a set of concentric rings, blocking signals arriving at low and negative elevation angles and having a low gain at these angles (Tranquilla, Carr & Al-Rizzo 1994). Antenna designs based on the signal polarization are widely used. The third method is related to the receiver itself, and the fourth one is related to the measurement post-processing, which deals with multipath-contaminated measurements. In this case, weighting schemes based on the elevation angle of the satellites or SNR measurements can be applied, the multipath error can be estimated based on observables combinations (see Section 2), and, if the receiver and its surroundings are static, the multipath error will repeat with every satellite orbit (Braasch 2017).

Over the past decades, studies have been conducted to assess the multipath effect on GNSS signals, including the four global constellations: Global Positioning System (GPS), GLONASS, Galileo and BeiDou (Breivik et al. 1997; Cai et al. 2016; Julg 1996; Kos, Markezic & Pokrajcic 2010; Prochniewicz & Grzymala 2021; Zhao et al. 2016). GPS and GLONASS, the pioneers, are currently going through modernizations, adding more capability and signals to their systems. Galileo is in the final stages of development, just a few steps away of becoming fully operational. It was designed with a new binary offset carrier (BOC)/alternative BOC (AltBOC) modulation, which provides greater resistance to short-range multipath as opposed to the GPS' and GLONASS' binary phase-shift keying (BPSK) modulation (Blunt 2009). BeiDou was declared operational in July 2020, with a full constellation of satellites transmitting signals in a quadrature phase-shift keying (QPSK) modulation.

As the multi-frequency and multi-constellation (MFMC) positioning offers a range of advantages compared to the GPS positioning (Kouba, Lahaye & Tétreault 2017; Montenbruck et al. 2017; Setti Júnior et al. 2020), the Brazilian Network for Continuous Monitoring of the GNSS Systems (RBMC – Rede Brasileira de Monitoramento Contínuo dos Sistemas GNSS), has been updating itself for a MCMF network. Currently, 48 stations track and record measurements from three or four of the global constellations. In this sense, this paper aims to assess and compare the impact of multipath on different frequencies and constellations observations and, thence, evaluate the multipath interference on RMBC MFMC stations. The code multipath combination based on the code-minus-carrier (CMC) combination was used in the analysis. The paper is organized as follows: Section 2 describes the process of obtaining an estimate of code multipath using the pseudorange and dual-frequency carrier-phase measurements; Section 3 presents the materials and method applied to the experiment; Section 4 describes the results and discussions; and, in Section 5, the conclusions and future work are presented.

2 Code Multipath Combination

To isolate the multipath impact on code observations when dual-frequency measurements are available, the CMC combination can be used. It is formulated on the basis of Equations 1 and 2 of the simplified code pseudorange and carrier-phase measurements (Braasch 2017):

$$PD = \rho + c(dt_r - dt^s) + I + T + M + E \quad \textbf{(1)}$$

$$\varphi = \rho + \lambda N + c(dt_r - dt^s) - I + T + m + \varepsilon \quad \textbf{(2)}$$

where PD is the code pseudorange, is φ the carrier-phase observation in meters, ρ is the receiver-satellite range, λ is the signal wavelength, N is the carrier-phase ambiguity, dt_r and dt^s are the receiver and satellite clock errors, respectively, I is the ionospheric delay, T is the tropospheric delay, M and m are the code and carrier-phase multipath error, respectively, E and ε and are the code and carrier phase measurement noise, respectively.

Equation 3, as demonstrated by Prochniewicz and Grzymala (2021), removes non-frequency related parameters such as geometric distance, clock, orbit, and tropospheric errors by subtracting Equation 2 from Equation 1:

$$PD - \varphi = -\lambda N + 2I + M + E - m - \varepsilon \quad \textbf{(3)}$$

The remaining parameters are the carrier-phase ambiguity, the doubled ionospheric delay, which affects the carrier-phase and the code observation with equal magnitude but with opposite signs, and the multipath error and measurement noise for both code and carrier-phase. As the carrier-phase multipath error and measurement noise are much smaller than the ones related to the code observations, they can be neglected. The CMC equation is then given by Equation 4 (Prochniewicz & Grzymala 2021):

$$CMC = M + E = PD - \varphi - 2I + \lambda N \quad \textbf{(4)}$$

The ambiguity parameter can be estimated by averaging the measurements in a connected phase arc, which is a set of continuous carrier-phase observations with no gaps or cycle slips. The ionospheric delay can be eliminated using double-frequency observations. Equations 5 and 6 provide a mean to convert the ionospheric delay at one frequency to a second frequency by:

$$I_j = \alpha I_i \quad \textbf{(5)}$$

where:

$$\alpha = \left(\frac{f_i}{f_j}\right)^2 \quad \textbf{(6)}$$

and f is the frequency of the signal, with subscripts i and j $(i \neq j)$ representing the carrier frequencies.

Equation 7 presents the formulation of the carrier-phase geometry-free combination φ_{GF} after eliminating the time constant ambiguity parameter:

$$\varphi_{GF} = \varphi_i - \varphi_j = I_i - I_j = I_i(\alpha - 1) \quad \textbf{(7)}$$

and, based on Equation 7, the ionospheric delay for L1 can be determined based on dual-frequency carrier-phase measurements by Equation 8:

$$I_i = \left(\frac{\varphi_i - \varphi_j}{\alpha - 1}\right) \quad \textbf{(8)}$$

The estimated ionospheric delay from Equation 8 can be applied in Equation 4, corrected from the carrier-phase ambiguity, obtaining in Equations 9 and 10 the CMC combination (Estey & Meertens 1999):

$$CMC_i = PD_i - \left(1 + \frac{2\alpha}{\alpha - 1}\right)\varphi_i + \left(\frac{2\alpha}{\alpha - 1}\right)\varphi_j \quad \textbf{(9)}$$

$$CMC_j = PD_j - \left(\frac{2\alpha}{\alpha - 1}\right)\varphi_i + \left(\frac{2\alpha}{\alpha - 1} - 1\right)\varphi_j \quad \textbf{(10)}$$

The CMC combination represents the estimated multipath for a given epoch. In some references (Cai et al. 2016; Pan, Guo & Ma 2018), the multipath error is referred to as code multipath and noises (CMN), as it is in fact a combination of the multipath and receiver noises, e.g., antenna and preamplifier noises, as well as remaining errors that are not completely eliminated in the geometry-free and ionosphere-free combinations. Alves et al. (2013), for example, showed that the estimated multipath is correlated to the ionospheric scintillation, especially in sites close to the magnetic equator.

3 Methodology

Out of the 48 RBMC MFMC stations that provide their observations in RINEX (Receiver Independent Exchange) 3 format, 35 of them are currently recording at least dual-frequency observations from the four global constellations; therefore, those 35 stations were selected for the experiment. Figure 1 presents their location. Table 1 presents the processed GPS, GLONASS, Galileo and BeiDou signals, along with their respective frequencies and number of tracked satellites. Regarding BeiDou constellation, most of the RBMC stations (Trimble NETR9 receiver) do not record the observations from more recent launchings (satellite number greater than 30), so most of the analysis are related to signals coming from 15 satellites; to the moment, only GOGY and PPTE (Trimble ALLOY receiver) stations are tracking 27 BeiDou satellites. One week of data (01 – 07 June 2021) was used in the experiment. The month of June was selected because it is the period when the ionospheric activity reaches its annual minimum and, therefore, its impact on the multipath estimates is minimized and does not severely impact our results.

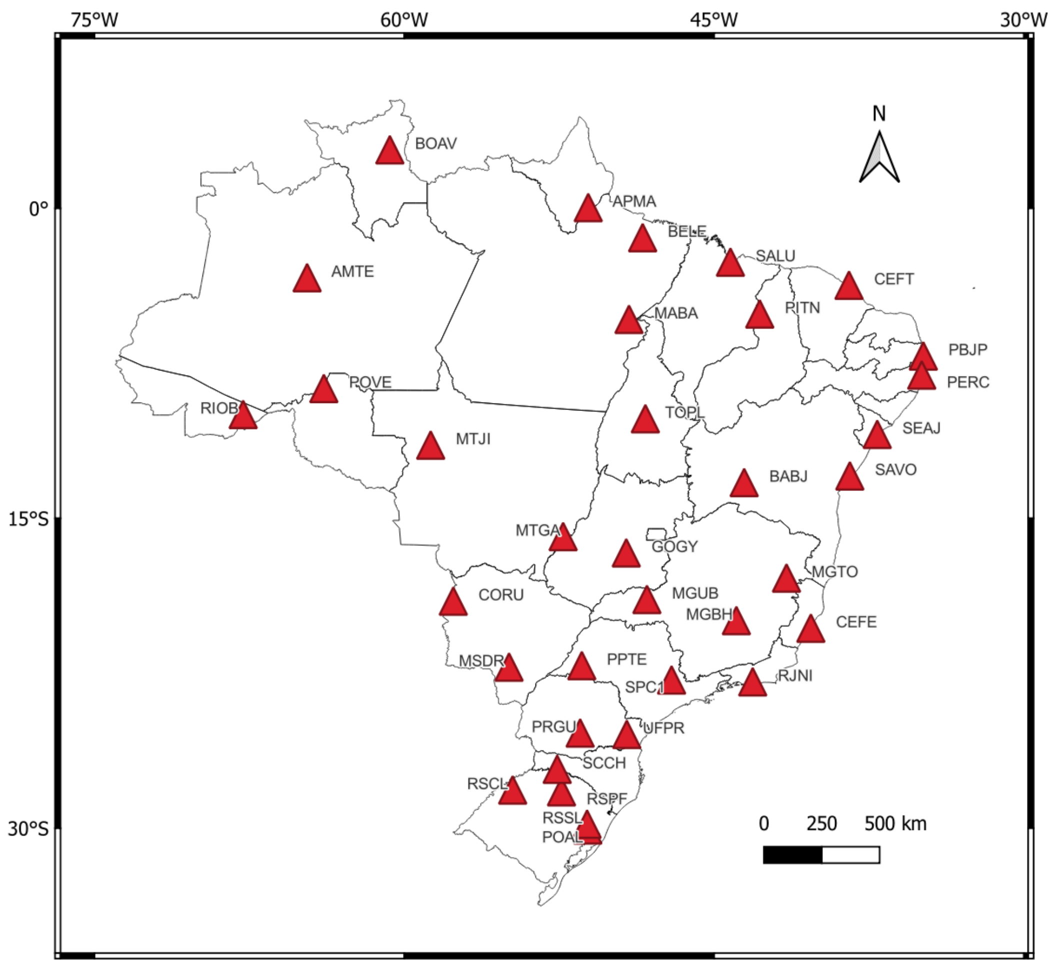

Figure 1 Location of selected RBMC stations.

Table 1 Selected signals.

System	Signal	Frequency (MHz)	Number of satellites
GPS	L1 C/A	1575.420	31
	L2P	1227.600	31
	L2C	1227.600	23
	L5	1176.450	16
GLONASS	G1	1602+0.5625k*	21
	G2	1246+0.4375k*	21
Galileo	E1	1575.420	24
	E5a	1176.450	24
	E5b	1207.140	24
	E5	1191.795	24
BeiDou	B1	1561.098	15/27
	B3	1268.520	15/27

*** k=** -7…+12

The code multipath was estimated using an in-house software developed by the authors, based on the CMC method described in Section 2, which is the same method used in the TEQC (Translation, Editing and Quality Checking) software (Estey & Meertens 1999), widely used for quality checking of GPS and GLONASS data. The ambiguities were estimated based on a 50-epoch averaging, considering a 15-second sample interval. To detect cycle slips, the TurboEdit method (Blewitt 1990) was used. The frequency combinations used in the experiment were (L1/L2P), (L2P/L1), (L2C/L1), (L5/L1), (G1/G2), (G2/G1), (E1/E5a), (E5a/E1), (E5b/E1), (E5/E1), (B1/B3), and (B3/B1). The results are analyzed in terms of the RMS of the multipath estimates considering all the stations, which is often referred to as the multipath index MP of a given signal. The elevation mask was set to 10° as observations below that threshold are very sensible to cycle slips, and the carrier-phase ambiguities cannot be well estimated and eliminated in the combination.

4 Results and Discussion

The results and discussion section is divided in two different parts. In the first one, the multipath impact on different frequencies and constellations is presented, compared, and discussed. In the second one, a comparison of the multipath effect in the selected RBMC stations is presented, highlighting some interesting findings regarding some of the stations.

4.1 MFMC Multipath Comparison

The code MP indices as a function of the satellite elevation angle, considering all 35 stations and 7 days of data, are presented in Figure 2. The RMS was calculated considering 10° elevation bins. Although the multipath error is particular to each station, averaging the results to all stations keeps the general behavior of each signal. Results for each individual station will be discussed in Subsection 4.2. For all constellations and frequencies, it is noted that the multipath decreases as the satellite elevation increases, which was already expected as the multipath error sources are on the ground. In the first frequency, GPS, GLONASS and BeiDou presented similar results, with GLONASS being slightly worse. Galileo, on the other hand, seems to be more resistant to multipath interference due to its BOC modulation: while the MP index, considering all elevation angles, was of 55 cm for GPS L1 C/A, of 57 cm for GLONASS G1 and of 56 cm for BeiDou B2, it was of 37 cm for Galileo E1 (Table 2).

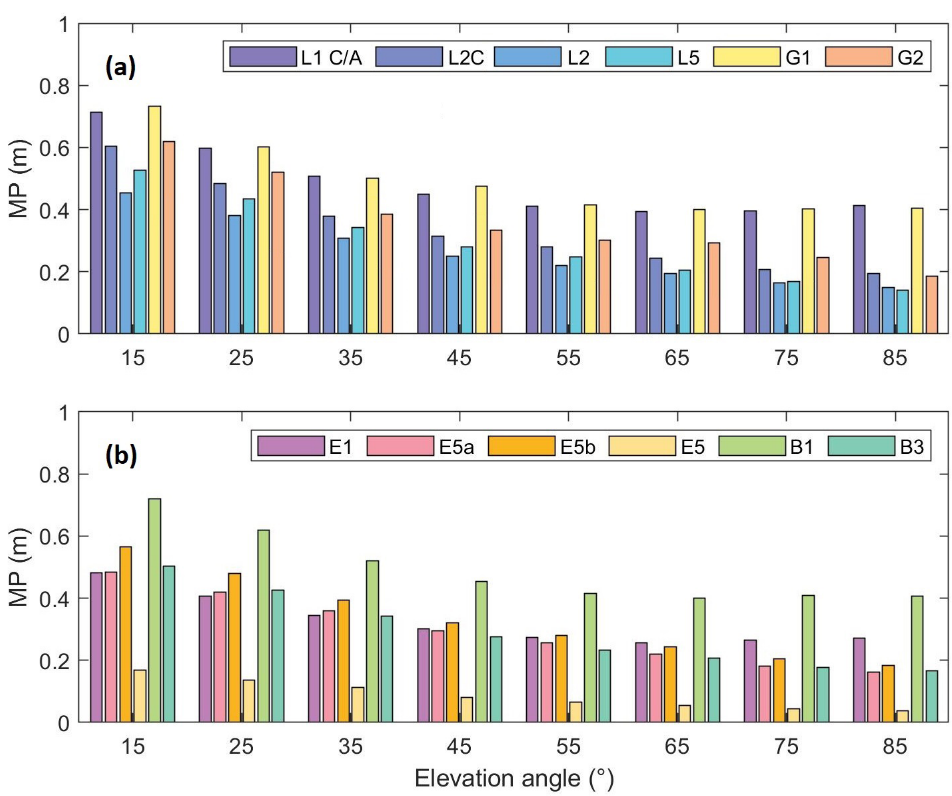

Figure 2 MP index versus elevation angle for: A. GPS and GLONASS signals; B: Galileo and BeiDou signals.

Table 2 MP index, considering selected period and stations.

Signal	**L1 C/A**	**L2C**	**L2P**	**L5**	**G1**	**G2**
MP (m)	0.55	0.44	0.34	0.38	0.57	0.47
Signal	**E1**	**E5a**	**E5b**	**E5**	**B1**	**B3**
MP (m)	0.37	0.37	0.42	0.12	0.56	0.37

Comparing the GPS frequencies, it is noted that L1 C/A and L2C were the ones with larger multipath error, especially at low elevation angles. The results show that the other two analyzed frequencies, L2P and L5, are less sensitive to the multipath effect. This fact can be explained by the chipping rate of these signals, which are higher than the ones from the civilian signals, making them much less sensitive to the indirect signals (Pratt 2009; Xu 2007). GLONASS G1 and G2 frequencies presented similar behaviors to those of GPS L1 and L2C signals, being slightly more affected by multipath due to the system's noisier FDMA (Frequency Division Multiple Access) technique.

Galileo E5a and E5b signals presented very similar results to the E1 frequency, with MP index of 37 cm and 42 cm, respectively. GPS L5 and Galileo E5a signals, transmitted at the same frequency, are affected by multipath in a similar magnitude. Considering all the frequencies and constellations, the signal with less multipath impact was Galileo E5, which is modulated by the AltBOC technique, with a RMS of 12 cm. The composite AltBOC signal offers a very large signal bandwidth, providing excellent multipath rejection (Falcone, Hahn & Burger 2017). Table 2 summarizes the multipath index for the selected periods and stations in the experiment.

As it is clear and obvious that the multipath impact is correlated to the satellite elevation angle, an estimate of the multipath error can be determined based on the elevation angle through a third-degree polynomial, as suggested by Prochniewicz and Grzymala (2021) and shown in Equation 11:

$$MP = a\theta^3 + b\theta^2 + c\theta + d \quad \textbf{(11)}$$

where θ is the elevation angle, and a, b, c and d are the estimated coefficients.

The third-degree polynomial was chosen due to its good fit to the data according to preliminary analyzes, with a R-squared value varying from 0.979 to 0.998, depending on the signal. The observations, binned at 5-degree satellite elevation intervals, and the adjusted curves are presented in Figure 3 for the different signals. Although the curves presented in this paper represent the average of all 35 selected stations, a different curve could be adjusted for the data of each station, and the results could be used or adapted, for example, as the stochastic model in GNSS positioning.

4.2 RBMC Stations Multipath Comparison

The comparative results presented and discussed in Subsection 4.1 regarding the different frequencies and constellations are valid for all the selected stations, with variations only in the index magnitude. As the continuously operating stations are installed in carefully selected locations, the multipath impact is usually not high. The GPS MP L1 C/A index for each station is presented in Figure 4, varying from 38 cm to 61 cm. Considering all 35 stations, the ones with higher MP index are APMA, CEFT, POVE, and AMTE. Stations CEFE, RJNI, and UFPR presented less multipath influence. The results for the other signals followed the same trend, with a correlation of 0.80 with GLONASS MP G1, of 0.82 with BeiDou MP B1, and of 0.87 with Galileo MP E1. As the multipath is highly impacted by the surrounding environment, no clear correlation was found between the index and the receiver and/or antenna type (Trimble NETR9 and Trimble ALLOY receivers, Zephyr 3 Geodetic and Zephyr GNSS Geodetic model 2 antennas).

When analyzing the data and results for this manuscript, some characteristics of the multipath behavior at BELE, POVE, and PPTE stations caught the authors' attention and are worth mentioning. Figure 5 shows the GPS L1 C/A and Galileo E1 multipath sky-plot of the three mentioned stations. From the images, it is clear the agreement between the results obtained using GPS and Galileo signals. The multipath index for the other signals followed the same behavior and their sky-plot are not shown. The three stations are strongly affected by multipath (up to 80 cm) in signals coming from the horizon, up to around 30° elevation angle, in at least some directions: BELE station from around 190° to 340° azimuth; POVE station from around 30° to 70° azimuth; and PPTE station from around 10° to 80° azimuth.

As an example of what is shown in Figure 5, Figure 6 depicts the location of PPTE station and its surrounding environment. Comparing the image with the sky-plot of the same station in Figure 5, one can note that the multipath effect in the region of 10° to 80° azimuth is caused by the natural vegetation around the station. The information presented and discussed here for the three selected stations could be used to improve the positioning performance on these stations. This can be done by adjusting the stochastic model and down-weighting observations coming from these regions, which are known to be more affected by the multipath effect.

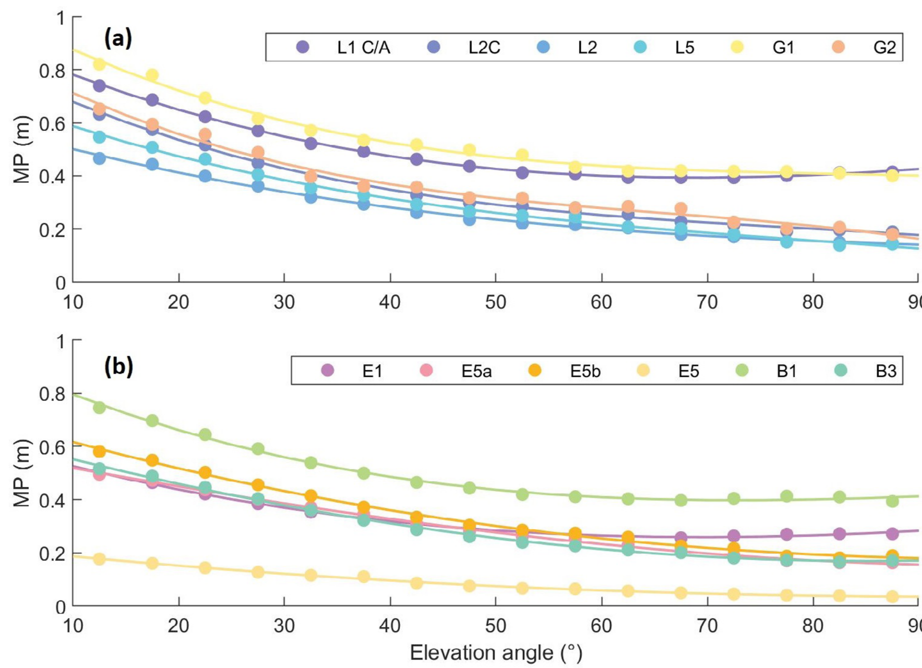

Figure 3 MP observations (dots) and modeled function (continuous lines), considering the elevation angle and signals from: A GPS and GLONASS; B. Galileo and BeiDou.

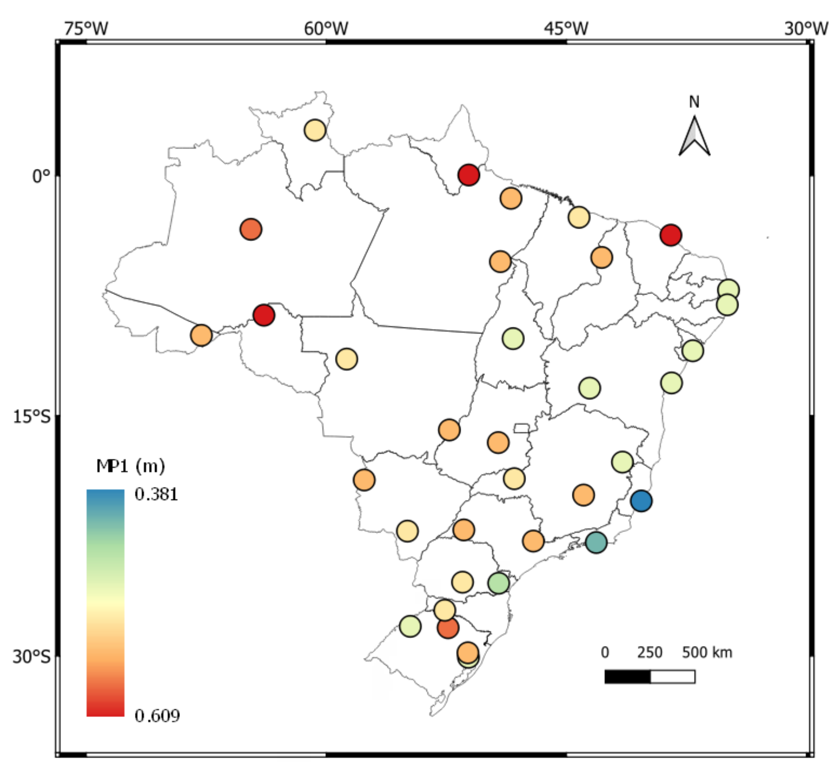

Figure 4 GPS L1 C/A MP for the selected RBMC stations.

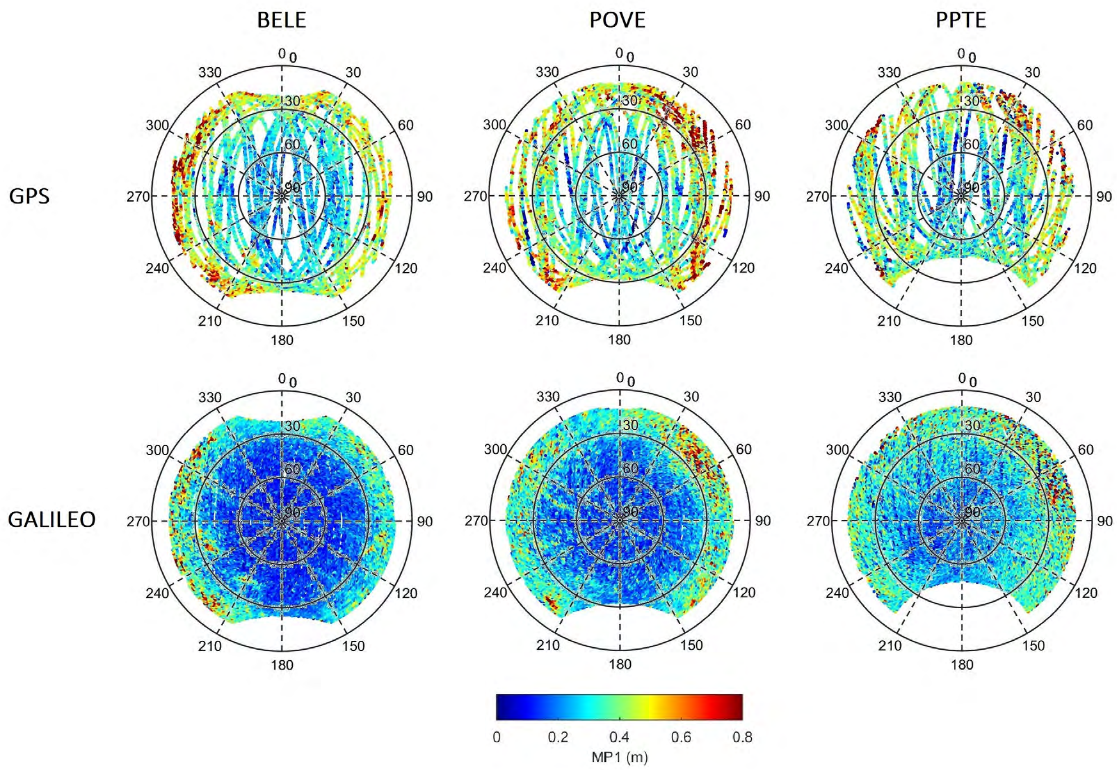

Figure 5 BELE, POVE and PPTE stations sky-plot, considering GPS and Galileo satellites.

Figure 6 PPTE station (red triangle) location and surrounding environment.

5 Conclusions

The impact of multipath effect on MFMC code observations was analyzed in this paper. A set of 35 stations from the RBMC and a period of 7 days in June 2021 were selected for the study. The code multipath was estimated based on the CMC combination. As expected, the results showed a dependency of the multipath on the incidence angle, with observations coming from low elevation angle satellites being more affected by the multipath. For the first frequency of each system, similar results were achieved for GPS, GLONASS and BeiDou (55 cm to 57 cm). Galileo, with its BOC modulation, seems to be less affected by the multipath effect, with a MP index of 37 cm for E1 signal, around 34% more resistant than the other three systems. The best results were obtained for Galileo E5 frequency (12 cm), with its AltBOC modulation, around 68% more resistant than Galileo E1 and 78% more resistant than GPS L1.

Considering the selected stations, the multipath in GPS L1 signal varied from around 40 cm to 60 cm, with similar results for the other constellations. This information, along with the sky-plot for some of the stations that were presented, can help readers to select the best stations when working with precise positioning (code observations are of great importance when estimating the float solution). It is important to highlight that what is referred to as “multipath index” in this paper is in fact a combination of the multipath error with some other errors and biases that are not completely eliminated in the geometry-free and ionosphere-free combinations.

Future work may include, but is not limited to, an analysis of how the detected multipath impacts the positioning performance of the different systems individually and in a combined way. It can be anticipated that, even though Galileo is less affected by multipath compared to the other systems, other effects may influence its positioning accuracy. GPS, for example, has more satellites in orbit, improving its dilution of precision (DOP) which, consequently, improves its positioning performance.

6 Acknowledgments

The authors would like to thank the National Council for Scientific and Technological Development (CNPq), file 304038/2020-2, the São Paulo Research Foundation (FAPESP), files 2021/08962-2, 2019/26669-0, and 2016/24861-3. The authors would also like to acknowledge the National Institute of Science and Technology (INCT) GNSS Technology for Supporting Air Navigation (GNSS-NavAer), funded by CNPq file 465648/2014-2 and FAPESP file 2017/01550-0.

7 References

Alves, D.B.M., Souza, E.M. de, Kaneshiro, V.Y. & Souza, J.S. 2013, ‘Análise de séries temporais de multicaminho em estações de monitoramento contínuo’, *Boletim de Ciências Geodésicas*, vol. 19, no. 3, pp. 353–73, DOI:10.1590/S1982-21702013000300001

Blewitt, G. 1990, ‘An automatic editing algorithm for GPS data’, *Geophysical Research Letters*, vol. 17, no. 3, pp. 199–202, DOI:10.1029/GL017i003p00199

Blunt, P. 2009, ‘GNSS Signal Acquisition and Tracking’, in S. Gleason & D. Gebre-Egziabher (eds), *GNSS applications and methods*, Artech House, Boston, pp. 23-54.

Braasch, M.S. 2017, ‘Multipath’, in P.J.G. Tenissen & O. Montenbruck (eds), *Springer Handbook of Global Navigation Satellite Systems.* Springer, Berlin, pp. 443-68.

Breivik, K., Forssell, B., Kee, C., Enge, P. & Walter, T. 1997, ‘Estimation of Multipath Error in GPS Pseudorange Measurements’, *Navigation*, vol. 44, no. 1, pp. 43–52, DOI:10.1002/j.2161-4296.1997.tb01938.x

Cai, C., He, C., Santerre, R., Pan, L., Cui, X. & Zhu, J. 2016, ‘A comparative analysis of measurement noise and multipath for four constellations: GPS, BeiDou, GLONASS and Galileo’, *Survey Review*, vol. 48, no. 349, pp. 287–95, DOI:10.1179/1752270615Y.0000000032

Estey, L. & Meertens, C.M. 1999, ‘TEQC: The Multi-Purpose Toolkit for GPS/GLONASS Data’, *GPS Solutions*, vol. 3, no. 1, pp. 42-9, DOI:10.1007/PL00012778

Falcone, M., Hahn, J. & Burger, T. 2017, ‘Galileo’, in P.J.G. Tenissen & O. Montenbruck (eds), *Springer Handbook of Global Navigation Satellite Systems*, Springer, Berlin, pp. 247-72.

Julg, T. 1996, ‘Evaluation of multipath error and signal propagation in a complex scenario for GPS multipath identification’, *Proceedings of ISSSTA’95 International Symposium on Spread Spectrum Techniques and Applications*, IEEE, Germany, pp. 872-6, vol. 2, DOI:10.1109/ISSSTA.1996.563248

Kos, T., Markezic, I. & Pokrajcic, J. 2010, ‘Effects of multipath reception on GPS positioning performance’, *Proceedings ELMAR-2010*, Croatia, pp. 399-402.

Kouba, J., Lahaye, F., Tétreault, P. 2017, ‘Precise Point Positioning’, in P.J.G. Tenissen & O. Montenbruck (eds), *Springer Handbook of Global Navigation Satellite Systems*, Springer, Berlin, pp. 723-52.

Montenbruck, O., Steigenberger, P., Prange, L., Deng, Z., Zhao, Q., Perosanz, F., Romero, I., Noll, C., Stürze, A., Weber, G., Schmid, R., MacLeod, K. & Schaer, S. 2017, ‘The Multi-GNSS Experiment (MGEX) of the International GNSS Service (IGS) – Achievements, prospects and challenges’, *Advances in Space Research*, vol. 59, no. 7, pp. 1671–97, DOI:10.1016/j.asr.2017.01.011

Pan, L., Guo, F. & Ma, F. 2018, 'An Improved BDS Satellite-Induced Code Bias Correction Model Considering the Consistency of Multipath Combinations', *Remote Sensing*, vol. 10, no. 18, e1189, DOI:10.3390/rs10081189

Pratt, A.R. 2009, 'New Navigation Signals and Future Systems in Evolution', in S. Gleason & D. Gebre-Egziabher (eds), *GNSS applications and methods*, Artech House, Boston, pp. 437-84.

Prochniewicz, D. & Grzymala, M., 2021. 'Analysis of the Impact of Multipath on Galileo System Measurements', *Remote Sensing*, vol. 13, no. 12, e2295, DOI:10.3390/rs13122295

Seeber, G., 2003, *Satellite geodesy*, 2nd edn, Walter de Gruyter, Berlin, New York.

Setti Júnior, P.T., Silva, C.M., Oliveira Júnior, P.S., Alves, D.B.M. & Monico, J.F.G. 2020, 'Posicionamento multi-GNSS', *Revista Brasileira de Cartografia*, vol. 72, pp. 1200–24, DOI:10.14393/rbcv72nespecial50anos-56580

Tranquilla, J.M., Carr, J.P. & Al-Rizzo, H.M. 1994, 'Analysis of a choke ring groundplane for multipath control in Global Positioning System (GPS) applications', *IEEE Transactions on Antennas and Propagation,* vol. 42, no. 7, pp. 905–11, DOI:10.1109/8.299591

Xu, G. 2007, *GPS: theory, algorithms, and applications*, 2nd edn, Springer, Berlin, New York.

Zhao, Q., Wang, G., Liu, Z., Hu, Z., Dai, Z. & Liu, J. 2016, 'Analysis of BeiDou Satellite Measurements with Code Multipath and Geometry-Free Ionosphere-Free Combinations', *Sensors*, vol. 16, no. 1, e123, DOI:10.3390/s16010123

Author contributions

Paulo T. Setti Jr.: conceptualization; formal analysis; methodology; validation; writing – original draft; writing review and editing. **Crislaine Menezes da Silva:** conceptualization; formal analysis; writing – original draft; writing review and editing. **Daniele Barroca Marra Alves:** conceptualization; formal analysis; methodology; writing review and editing; supervision. **João Vitor Espinhosa Vieira:** methodology; validation. **João Pedro Voltare Zaupa:** methodology; validation.

Conflict of interest

The authors declare no conflict of interest.

Data availability statement

All data included in this study are publicly available in the literature.

Funding information

CNPq, Process Nº 304038/2020-2.
FAPESP, Process Nº 2021/08962-2; 2019/26669-0; 2016/24861-3.

Editor-in-chief

Dr. Claudine Dereczynski

Associate Editor

Dr. Martim Moultom

How to cite:

Setti JR., P.T., Silva, C.M., Alves, D.B.M., Vieira, J.V.E. & Zaupa, J.P.V. 2023, 'Multipath Impact on Multi-Frequency and Multi-Constellation Code Measurements from Brazilian GNSS Stations', *Anuário do Instituto de Geociências,* 46:53216. https://doi.org/10.11137/1982-3908_2023_46_53216